OPT2022: 14th Annual Workshop on Optimization for Machine Learning

Exact Gradient Computation for Spiking Neural Networks

Jane H. Lee JANE.H.LEE@YALE.EDU
New Haven, CT, USA

Saeid Haghighatshoar SAEID.HAGHIGHATSHOAR@SYNSENSE.AI
Zurich, Switzerland

Amin Karbasi AMIN.KARBASI@YALE.EDU
New Haven, CT, USA

Abstract

Spiking neural networks (SNNs) have recently emerged as an alternative to traditional neural networks, holding promise for energy efficiency benefits. However, the classic backpropagation algorithm for training traditional networks has been notoriously difficult to apply to SNNs due to the hard-thresholding and discontinuities at spike times. Therefore, a large majority of prior work believes that exact gradients for SNN w.r.t. their weights do not exist and has focused on approximation methods to produce surrogate gradients. In this paper, (1) by applying the implicit function theorem to SNN at the discrete spike times, we prove that, albeit being non-differentiable in time, SNNs have well-defined gradients w.r.t. their weights, and (2) we propose a novel training algorithm, called *forward propagation* (FP), that computes exact gradients for SNNs. Our derivation of FP in this paper provides insights on why other related algorithms such as Hebbian learning and also recently-proposed surrogate gradient methods may perform well.

Keywords: first order methods, neuromorphic computing, spiking neural networks

1. Introduction

Spiking neural networks (SNNs), inspired by biological neuronal mechanisms and sometimes referred to as the third generation of neural networks [31], have garnered considerable attention recently [7, 9, 11, 35, 37] as low-power alternatives. Indeed, SNNs have been shown to yield 1-2 orders of magnitude energy saving over ANNs on emerging neuromorphic hardware [1, 10]. SNNs have other unique properties, owing to their ability to model biological mechanisms such as dendritic computations with temporally evolving potentials [17] or short-term plasticity, which allow them to even outperform ANNs in accuracy in some tasks [32]. The power of neuromorphic computing can even be seen in ANNs, e.g., [21] use rank-coding in ANN inspired by the temporal encoding of information in SNNs. However, due to the discontinuous resetting of the membrane potential in spiking neurons, e.g., in Integrate-and-Fire (IF) or Leaky-Integrate-and-Fire (LIF) type neurons [6, 24], it is notoriously difficult to calculate gradients and train SNNs by conventional methods. For instance, the authors of [21] note "spike coding poses difficulties and training that require ad hoc mitigation" and "SNNs are particularly difficult to analyse mathematically". As such, many works focus on how to train SNN without exact gradients, which range from heuristic rules like in Hebbian learning [23, 39] and STDP [28, 30], or other methods like SNN-ANN conversion [12, 19, 38] and surrogate gradient approximations [34].

In this work, by applying the implicit function theorem (IFT) at the firing times of the neurons in SNN, we first show that under fairly general conditions, gradients of loss w.r.t. network weights are well-defined. We do this by proving that the conditions for IFT are always satisfied at firing times. We then provide what we call a *forward-propagation* (FP) algorithm which uses the causality structure in network firing times and our IFT-based gradient calculations in order to calculate exact gradients of the loss w.r.t. network weights. We call it forward propagation because intermediate calculations needed to calculate the final gradient are actually done forward in time (or forward in layers for feed-forward networks). We highlight the following features of our method:

- Our method can be applied in networks with arbitrary recurrent connections (up to self loops) and is agnostic to how the forward pass is implemented.
- Our method can be seen as an extension of Hebbian learning as it illustrates that the gradient w.r.t. a weight W_{ji} connecting neuron j to neuron i is almost an average of the feeding kernel y_{ji} between these neurons at the firing times. In the context of Hebbian learning (especially from a biological perspective), this is interpreted as the well-known fact that *stronger feeding/activation amplifies the association between the neurons.* [8, 16]
- In our method, the smoothing kernels y_{ji} arise naturally as a result of application of IFT at the firing times, resembling the smoothing kernels applied in surrogate gradient methods. As a result, (1) our method sheds some light on why the surrogate gradient methods may work quite well, and (2) in our method, the smoothing kernels y_{ji} vary according to the firing times between two neurons; thus, they can be seen as an adaptive version of the fixed smoothing kernels used in surrogate gradient methods. See remark 2.

1.1. Related Work

A review of learning in deep spiking networks can be found at [36, 37, 43, 44], with [37] discussing also developments in neuromorphic computing in both software (algorithms) and hardware. [34] focuses on surrogate gradient methods, which use smooth activation functions in place of the hard-thresholding for compatibility with usual backpropagation and have been used to train SNNs in a variety of settings [3, 14, 20, 40, 42, 46].

A number of works explore backpropagation in SNNs [5, 22, 47]. The SpikeProp [5] framework assumes a linear relationship between the "post-synaptic input and the resultant spiking time," which our framework does not rely on. The method in [22] and its RSNN version [47] are limited to a rate-coded loss that depends on spike counts. The continuous "spike time" representation of spikes in our framework is related to temporal coding [33], but the authors of [33] in the context of differentiation of losses largely ignore the discontinuities that occur at spikes times, stating "the derivative...is discontinuous at such points...[but] many feedforward ANNs use activation functions with a discontinuous first derivative...". In contrast with [33], we prove that exact gradients can be calculated despite this discontinuity.

As mentioned in [45], applying methods from optimal control theory to compute exact gradients in hard-threshold spiking neural networks has already been recognized [26, 27, 41]. However, unlike in our setting these works consider a neuron with a two-sided threshold and provide specialized algorithms for specific loss functions. Our work, as well as these works which compute exact gradients for SNNs, share in common the application of the implicit function theorem to differentiate spike times w.r.t. synaptic weights. Most related to our work is the recent EventProp [45] which

derives an algorithm for a continuous-time spiking neural network by applying the adjoint method (which can be seen as generalized backpropagation) together with proper partial derivative jumps.

2. Spiking Neural Networks

In this section, we first describe the precise models we use throughout the paper for the pre-synaptic and post-synaptic behaviors of spiking neurons. We then explain the dynamics of a SNN and the effects of spike generations. For the remainder of the paper, we consider SNN architectures up to arbitrary recurrent connections between neurons.

2.1. Post-Synaptic Kernel Model

We call the model illustrated in the left of Fig. 1 the pre-synaptic model. See Appendix A.1 for details. In this paper, we will work with a modified but equivalent model in which we combine the synaptic and neuron dynamics, and consider the effect of spiking dynamics of $\mathcal{N}_i$ directly on the membrane potential after it is being smoothed out by the synapse and neuron low-pass filters. We call this the post-synaptic or kernel model of the SNN.

To derive this model, we simply use the fact that the only source of non-linearity in SNN is hard-thresholding during the spike generation. And, in particular, SNN dynamics from the stimulating neuron $j \in \mathcal{N}_i$ until the membrane potential $V_i(t)$ is completely linear and can be described by the joint impulse response

$$h_{ji}(t) = h_j^s(t) \star h_i^n(t) = \int_{-\infty}^{\infty} h_j^s(\tau) h_i^n(t-\tau) d\tau = \int_0^t e^{-\alpha_j \tau} e^{-\beta_i (t-\tau)} d\tau = \frac{e^{-\alpha_j t} - e^{-\beta_i t}}{\beta_i - \alpha_j} u(t). \tag{1}$$

Therefore the whole effect of spikes $\mathcal{F}_j$ of neuron $j \in \mathcal{N}_i$ on the membrane potential can be written in terms of kernel $y_{ji}(t) = \sum_{f \in \mathcal{F}_j} h_{ji}(t-f)$. We call this model post-synaptic since the effect of dynamic of neuron $j \in \mathcal{N}_i$ on $V_i(t)$ is considered after being processed by the synapse and even the neuron i. Using the linearity and applying super-position for linear systems, we can see that the effect of all spikes coming for all stimulating neurons $\mathcal{N}_i$, can be written as

$$V_i^{\circ}(t) = \sum_{j \in \mathcal{N}_i} W_{ji} y_{ji}(t), \tag{2}$$

where W_{ji} is the weight from neuron j to i. We used $V_i^{\circ}(t)$ to denote the contribution to the membrane potential $V_i(t)$ after neglecting the potential reset due to hard-thresholding and spike generation. Fig. 1 (right) illustrates the post-synaptic model for the SNN.

Remark 1 *Our main motivation for using this equivalent model comes from the fact that even though the spikes are not differentiable functions, the effect of each stimulating neuron $j \in \mathcal{N}_i$ on neuron i is written as a well-defined and (almost everywhere) differentiable kernel $y_{ji}(.)$.* $\lozenge$

Remark 2 (Connection with the surrogate gradients) *Intuitively speaking, and as we will show rigorously in the following sections, the kernel model derived here immediately shows that SNNs have an intrinsic smoothing mechanism for their abrupt spiking inputs, through the low-pass impulse response $h_{ji}(t)$ between their neurons. As a result, one does not need to introduce any additional artificial smoothing to derive surrogate gradients by modifying the neuron model in the*

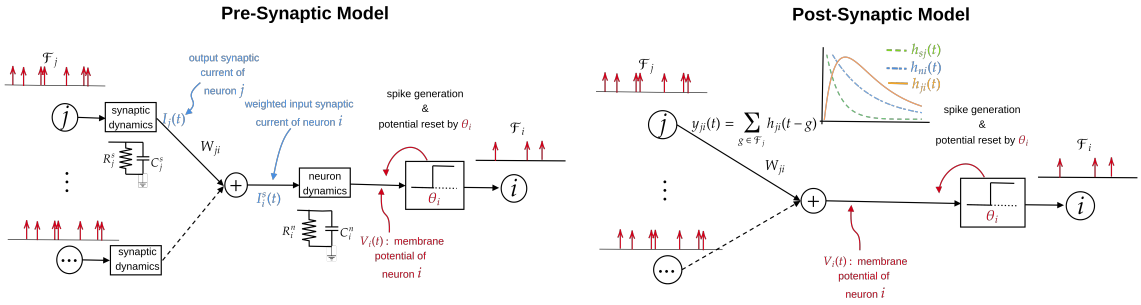

Figure 1: **(Left)** Generic structure of SNN. **(Right)** Post-synaptic kernel model of SNN. In this model neuron $j \in \mathcal{N}_i$ stimulates neuron i through the smooth kernel $y_{ji}(t) = \sum_{g\in\mathcal{F}_i} h_{ji}(t-g)$ rather than the abrupt spiking signal $\sum_{g\in\mathcal{F}_j} \delta(t-g)$. Thm. 3 shows equivalence of both models in computing membrane potentials.

backward gradient computation path. We will use this inherent smoothing to prove that SNNs indeed have well-defined gradients. Interestingly, our derivation of the exact gradient based on this inherent smoothing property intuitively explains that even though surrogate gradients are not exact, they may be close to and yield a similar training performance as the exact gradients. ◊

2.2. SNN Full Dynamics

In the post-synaptic kernel model, we already specified the effect of spikes from stimulating neurons as in (2). To have a full picture of the SNN dynamics, we need to specify also the effect of spike generation. The following theorem completes this.

Theorem 3 *Let i be a generic neuron in SNN and let $\mathcal{N}_i$ be the set of its stimulating neurons. Let $h_i^n(t)$ and $h_j^s(t)$ be the impulse response of the neuron i and synapse $j \in \mathcal{N}_i$, respectively, and let $h_{ji}(t) = h_i^n(t) \star h_j^s(t)$. Then the membrane potential of the neuron i for all times t is given by*

$$V_i(t) = V_i^\circ(t) - \sum_{f\in\mathcal{F}_i} \theta_i h_i^n(t-f), \tag{3}$$

where $y_{ji}(t) = \sum_{g\in\mathcal{F}_j} h_{ji}(t-g)$ denotes the smoothed kernel between the neuron i and $j \in \mathcal{N}_i$, and θ_i denotes the spike generation threshold of the neuron i.

Proof is provided in the Appendix A.2, A.3.

3. Exact Gradient Computation via Implicit Function Theorem

The Implicit Function Theorem (IFT) will be our main tool for proving the existence of gradients for SNNs. A full statement of the theorem and examples are given in the Appendix A.4.

3.1. Loss Formulation in SNNs

To use IFT, we need to specify the loss function used for training. In most settings, we feed the network with an input signal consisting of a collection of spikes within a given time interval and

record the firing times $\mathcal{F} = \sqcup_i \mathcal{F}_i$ (disjoint union) of all the spikes produced by neurons i and also the potential of the output layer $V_o(t)$. Here, we consider a quite generic loss function of the form

$$\mathcal{L} = \ell_{\mathcal{F}}(\mathcal{F}; W) + \int_0^T \ell_V(V_o(t), \mathcal{F}; W)\mathrm{dt}, \tag{4}$$

where $\ell_{\mathcal{F}}$ and ℓ_V are assumed to be differentiable functions of all their arguments, with $\ell_{\mathcal{F}}$ the part of the loss that depends on firing times $\mathcal{F}$, and ℓ_V the part that depends on membrane potential at the output layer, respectively. Note the second term $\ell_V(V_o(t), \mathcal{F}; W)$ is typically relevant in regression tasks, where in those cases we always assume that the output layer is linear without any firing and potential reset. The first term, in contrast, typically happens in classification tasks.

Theorem 4 *Let $\mathcal{L}$ be the generic loss function as defined before in (4). Then,*

(i) loss $\mathcal{L}$ depends only on the spike firing times $\mathcal{F}$ and the weights W, i.e., $\mathcal{L} = \mathcal{L}(\mathcal{F}, W)$,

(ii) $\mathcal{L}(\mathcal{F}, W)$ is a differentiable function of $\mathcal{F}$ and W if $\ell_V(V_o(t), \mathcal{F}; W)$ and $\ell_{\mathcal{F}}(\mathcal{F}; W)$ are differentiable functions of all their arguments $(V_o(t), \mathcal{F}; W)$,

(iii) loss $\mathcal{L}$ has well-defined gradients w.r.t. the weights W if the spike firing times $\mathcal{F}$ are differentiable w.r.t. the weights W.

The proof is provided in Appendix A.5. Theorem 4 implies that to prove the existence of the gradients w.r.t. to the weights, which is needed for training the SNN, it is sufficient to prove that the firing times $\mathcal{F}$ are differentiable w.r.t. the weights W. We will prove this in the next section by applying the IFT.

3.2. Differentiability of Firing Times w.r.t. Weights

Let us consider a generic neuron i and let us write the set of equations for firing times of i by using (8) as:

$$V_i(f) = \sum_{j \in \mathcal{N}_i} W_{ji} y_{ji}(f) - \theta_i \sum_{m<f} h_i^n(f-m) - \theta_i = 0, \tag{5}$$

where with some abuse of notation we use f both for the firing time and its label $(i, f) \in \mathcal{F} = \sqcup_l \mathcal{F}_l$. We can write the equations for all the firing times as $\mathbb{V}(\mathcal{F}, W) = \mathbf{0}$ where $\mathbb{V} : \mathbb{R}^{\mathsf{F}} \times \mathbb{R}^{\mathsf{W}} \to \mathbb{R}^{\mathsf{F}}$ is the nonlinear mapping connecting the F firing times and W weight parameters.

Theorem 5 *Let $\mathbf{P}$ be a permutation matrix sorting the firing times in $\mathcal{F}$ in an ascending order. Then, $\frac{\partial \mathbb{V}}{\partial \mathcal{F}} = \mathbf{P}^T \mathbf{L} \mathbf{P}$ where $\mathbf{L}$ is an $\mathsf{F} \times \mathsf{F}$ lower triangular matrix. Moreover, $\mathbf{L}$ has strictly positive diagonal elements $\mathbf{L}_{kk} > 0$ for all $k = 1, 2, \ldots, \mathsf{F}$.*

Proof We note that due to causality (future firing times cannot affect past ones), the equation corresponding to a specific firing time $f \in \mathcal{F}$ can only have contribution from firing times less than f. In other words, $\frac{\partial V_f}{\partial g} = 0$ for all $g < f$. Letting $\mathbf{P}$ be the permutation matrix sorting the firing times, therefore, the Jaccobian matrix of the sorted firing times given by $\mathbf{P} \frac{\partial \mathbb{V}}{\partial \mathcal{F}} \mathbf{P}^T$ should be a lower triangular matrix $\mathbf{L}$. This yields the first part $\frac{\partial \mathbb{V}}{\partial \mathcal{F}} = \mathbf{P}^T \mathbf{L} \mathbf{P}$. To check the second part, let k be the

index of a specific firing time f in the sorted version. Let us denote the neuron corresponding to the firing f by i. Then, we have that

$$\mathbf{L}_{kk} = \frac{\partial \mathbb{V}_f}{\partial f} = \frac{d}{df} V_i(f)\Big|_{\text{all other firing times fixed}} = V_i'(t)\Big|_{t=f^-} > 0$$

which is equal to the left time derivative the potential $V_i(t)$ when it passes through the threshold θ_i at time $t = f$. It is worthwhile to mention that that since $V_i(f)$ is a differentiable function of f, it has both left and right derivatives and they are equal. However, this derivative is equal to only the left derivative of the potential. Note that this derivative should be strictly positive otherwise the potential will not surpass the firing threshold θ_i and no firing time will happen. This completes the proof. ■

Using Theorem 5, we can now prove that the conditions of IFT (Theorem 6) are always fulfilled for firing time equations. This give us explicit formulas for the gradients of the network firing times w.r.t. network weights (Theorem 9). This is summarized in the following theorem.

Theorem 6 *Let $\mathbb{V}(\mathcal{F}, W) = \mathbf{0}$ be the set of equations corresponding to the firing times. Then the $\mathsf{F} \times \mathsf{F}$ Jacobian matrix $\frac{\partial \mathbb{V}}{\partial \mathcal{F}}$ is non-singular. Moreover, the firing times $\mathcal{F}$ can be written as a differentiable function of the weights W.*

Proof The first part result follows from Theorem 5:

$$\det\left(\frac{\partial \mathbb{V}}{\partial \mathcal{F}}\right) = \det(\mathbf{P}^T\mathbf{L}\mathbf{P}) = \det(\mathbf{P})\det(\mathbf{L})\det(\mathbf{P}^T) = \det(\mathbf{L}) = \prod_k \mathbf{L}_{kk} > 0,$$

where we used the fact that $\det(\mathbf{P}) = 1$ for any permutation matrix $\mathbf{P}$. The second part follows from Implicit Function Theorem: $\mathbb{V}(\mathcal{F}, W)$ is a differentiable function of the firing times and weights and $\frac{\partial \mathbb{V}}{\partial \mathcal{F}}$ is non-singular, thus, firing times $\mathcal{F}$ can be written as a differentiable function of the weights. ■

Remark 7 *Using Theorem 5 and 6 and applying the IFT, we have that $\frac{\partial \mathbb{V}}{\partial \mathcal{F}} \times \frac{\partial \mathcal{F}}{\partial W} = -\frac{\partial \mathbb{V}}{\partial W}$. After suitable sorting of the firing times $\mathcal{F}$ (thus, setting the required permutation matrix $\mathbf{P}$ to the identity matrix), this can be written as*

$$\mathbf{L}\frac{\partial \mathcal{F}}{\partial W} = -\frac{\partial \mathbb{V}}{\partial W}, \tag{6}$$

where $\mathbf{L}$ is a lower diagonal matrix. As a result, one can solve for the derivatives $\frac{\partial \mathcal{F}}{\partial W}$ recursively, so no matrix inversion is needed. ◊

Remark 8 *The matrix $\frac{\partial \mathbb{V}}{\partial W}$ depends only on the values of kernels at the firing times. More specifically, let f be a firing times of neuron i and let $j \in \mathcal{N}_i$ be one of the feeding neurons of neuron i. Then, $\frac{\partial \mathbb{V}(f)}{\partial W_{ji}} = y_{ji}(f)$. Moreover, $\frac{\partial \mathbb{V}(f)}{\partial W_{kl}} = 0$ if $l \neq i$ or $k \notin \mathcal{N}_i$.* ◊

Theorem 9 *(Existence of gradients w.r.t. weights) Let $\mathcal{L}$ be a generic loss function for training a SNN as in (4) with ℓ_V and $\ell_{\mathcal{F}}$ being differentiable w.r.t. their arguments. Then, $\mathcal{L}$ has well-defined gradients w.r.t. weights.*

Proof From Theorem 4, $\mathcal{L}$ has well-defined gradients w.r.t. weights if the firing times $\mathcal{F}$ are differentiable w.r.t. weights, which follows from Theorem 6 by applying the IFT. This completes the proof. ■

4. Discussion

Our framework offers an alternative view of the differentiability of SNN w.r.t. network weights and provides a new algorithm, forward-propagation (FP) to calculate gradients of SNN by accumulating information in the forward pass of the network. Implementation details are in Appendix A.7. Our results apply very generally to networks with arbitrary recurrent connections, and the FP algorithm can even be used with other algorithms that can simulate the continuous time dynamics in the forward pass. The effect of training SNN with exact gradients, as opposed to surrogate gradients as used in practice, can be seen in practice: using exact gradients results in faster convergence and steeper decrease in the loss function as shown in empirical experiments in Appendix A.8.

References

[1] Filipp Akopyan, Jun Sawada, Andrew Cassidy, Rodrigo Alvarez-Icaza, John Arthur, Paul Merolla, Nabil Imam, Yutaka Nakamura, Pallab Datta, Gi-Joon Nam, Brian Taba, Michael Beakes, Bernard Brezzo, Jente B. Kuang, Rajit Manohar, William P. Risk, Bryan Jackson, and Dharmendra S. Modha. Truenorth: Design and tool flow of a 65 mw 1 million neuron programmable neurosynaptic chip. *IEEE Transactions on Computer-Aided Design of Integrated Circuits and Systems*, 34(10):1537–1557, 2015. doi: 10.1109/TCAD.2015.2474396.

[2] Edgar Anderson. The species problem in iris. *Annals of the Missouri Botanical Garden*, 23(3): 457–509, 1936. ISSN 00266493. URL http://www.jstor.org/stable/2394164.

[3] Guillaume Bellec, Darjan Salaj, Anand Subramoney, Robert Legenstein, and Wolfgang Maass. Long short-term memory and learning-to-learn in networks of spiking neurons. In S. Bengio, H. Wallach, H. Larochelle, K. Grauman, N. Cesa-Bianchi, and R. Garnett, editors, *Advances in Neural Information Processing Systems*, volume 31. Curran Associates, Inc., 2018. URL https://proceedings.neurips.cc/paper/2018/file/c203d8a151612acf12457e4d67635a95-Paper.pdf.

[4] Yoshua Bengio, Nicholas Léonard, and Aaron Courville. Estimating or propagating gradients through stochastic neurons for conditional computation, 2013. URL https://arxiv.org/abs/1308.3432.

[5] Sander M. Bohté, Joost N. Kok, and Han La Poutré. Spikeprop: backpropagation for networks of spiking neurons. In *ESANN*, 2000.

[6] Anthony Burkitt. A review of the integrate-and-fire neuron model: I. homogeneous synaptic input. *Biological cybernetics*, 95:1–19, 08 2006. doi: 10.1007/s00422-006-0068-6.

[7] Yongqiang Cao, Yang Chen, and Deepak Khosla. Spiking deep convolutional neural networks for energy-efficient object recognition. *International Journal of Computer Vision*, 113:54–66, 05 2015. doi: 10.1007/s11263-014-0788-3.

[8] Yoonsuck Choe. *Hebbian Learning*, pages 1–5. Springer New York, New York, NY, 2013. ISBN 978-1-4614-7320-6. doi: 10.1007/978-1-4614-7320-6_672-1. URL https://doi.org/10.1007/978-1-4614-7320-6_672-1.

[9] Iulia Comsa, Thomas Fischbacher, Krzysztof Potempa, Andrea Gesmundo, Luca Versari, and Jyrki Alakuijala. Temporal coding in spiking neural networks with alpha synaptic function. pages 8529–8533, 05 2020. doi: 10.1109/ICASSP40776.2020.9053856.

[10] Mike Davies, Narayan Srinivasa, Tsung-Han Lin, Gautham Chinya, Yongqiang Cao, Sri Harsha Choday, Georgios Dimou, Prasad Joshi, Nabil Imam, Shweta Jain, Yuyun Liao, Chit-Kwan Lin, Andrew Lines, Ruokun Liu, Deepak Mathaikutty, Steven McCoy, Arnab Paul, Jonathan Tse, Guruguhanathan Venkataramanan, Yi-Hsin Weng, Andreas Wild, Yoonseok Yang, and Hong Wang. Loihi: A neuromorphic manycore processor with on-chip learning. *IEEE Micro*, 38(1):82–99, 2018. doi: 10.1109/MM.2018.112130359.

[11] Peter Diehl and Matthew eCook. Unsupervised learning of digit recognition using spike-timing-dependent plasticity. *Frontiers in Computational Neuroscience*, 9, 08 2015. doi: 10.3389/fncom.2015.00099.

[12] Jianhao Ding, Zhaofei Yu, Yonghong Tian, and Tiejun Huang. Optimal ann-snn conversion for fast and accurate inference in deep spiking neural networks. *ArXiv*, abs/2105.11654, 2021.

[13] Jason K Eshraghian, Max Ward, Emre Neftci, Xinxin Wang, Gregor Lenz, Girish Dwivedi, Mohammed Bennamoun, Doo Seok Jeong, and Wei D Lu. Training spiking neural networks using lessons from deep learning. *arXiv preprint arXiv:2109.12894*, 2021.

[14] Steven K. Esser, Paul A. Merolla, John V. Arthur, Andrew S. Cassidy, Rathinakumar Appuswamy, Alexander Andreopoulos, David J. Berg, Jeffrey L. McKinstry, Timothy Melano, Davis R. Barch, Carmelo di Nolfo, Pallab Datta, Arnon Amir, Brian Taba, Myron D. Flickner, and Dharmendra S. Modha. Convolutional networks for fast, energy-efficient neuromorphic computing. *Proceedings of the National Academy of Sciences*, 113(41):11441–11446, 2016. ISSN 0027-8424. doi: 10.1073/pnas.1604850113. URL https://www.pnas.org/content/113/41/11441.

[15] R. A. Fisher. The use of multiple measurements in taxonomic problems. *Annals of Eugenics*, 7(2):179–188, 1936. doi: https://doi.org/10.1111/j.1469-1809.1936.tb02137.x. URL https://onlinelibrary.wiley.com/doi/abs/10.1111/j.1469-1809.1936.tb02137.x.

[16] Wulfram Gerstner, Werner M. Kistler, Richard Naud, and Liam Paninski. *Neuronal Dynamics: From Single Neurons to Networks and Models of Cognition*. Cambridge University Press, 2014. doi: 10.1017/CBO9781107447615.

[17] Albert Gidon, Timothy Adam Zolnik, Pawel Fidzinski, Felix Bolduan, Athanasia Papoutsi, Panayiota Poirazi, Martin Holtkamp, Imre Vida, and Matthew Evan Larkum. Dendritic action potentials and computation in human layer 2/3 cortical neurons. *Science*, 367(6473):83–87, 2020. doi: 10.1126/science.aax6239. URL https://www.science.org/doi/abs/10.1126/science.aax6239.

[18] Julian Göltz, Laura Kriener, Andreas Baumbach, Sebastian Billaudelle, Oliver Breitwieser, Benjamin Cramer, Dominik Dold, Akos Ferenc Kungl, Walter Senn, Johannes Schemmel, Karlheinz Meier, and Mihai Alexandru Petrovici. Fast and energy-efficient neuromorphic deep learning with first-spike times, 2021.

[19] Nguyen-Dong Ho and Ik-Joon Chang. Tcl: an ann-to-snn conversion with trainable clipping layers. In *2021 58th ACM/IEEE Design Automation Conference (DAC)*, pages 793–798, 2021. doi: 10.1109/DAC18074.2021.9586266.

[20] Dongsung Huh and Terrence J Sejnowski. Gradient descent for spiking neural networks. In S. Bengio, H. Wallach, H. Larochelle, K. Grauman, N. Cesa-Bianchi, and R. Garnett, editors, *Advances in Neural Information Processing Systems*, volume 31. Curran Associates, Inc., 2018. URL https://proceedings.neurips.cc/paper/2018/file/185e65bc40581880c4f2c82958de8cfe-Paper.pdf.

[21] Alan Jeffares, Qinghai Guo, Pontus Stenetorp, and Timoleon Moraitis. Spike-inspired rank coding for fast and accurate recurrent neural networks. In *International Conference on Learning Representations*, 2022. URL https://openreview.net/forum?id=iMH1e5k7n3L.

[22] Yingyezhe Jin, Wenrui Zhang, and Peng Li. Hybrid macro/micro level backpropagation for training deep spiking neural networks. In S. Bengio, H. Wallach, H. Larochelle, K. Grauman, N. Cesa-Bianchi, and R. Garnett, editors, *Advances in Neural Information Processing Systems*, volume 31. Curran Associates, Inc., 2018. URL https://proceedings.neurips.cc/paper/2018/file/3fb04953d95a94367bb133f862402bce-Paper.pdf.

[23] Richard Kempter, Wulfram Gerstner, and Leo van Hemmen. Hebbian learning and spiking neurons. *Phys. Rev. E*, 59, 04 1999. doi: 10.1103/PhysRevE.59.4498.

[24] Vladimir Kornijcuk, Hyungkwang Lim, Jun Yeong Seok, Guhyun Kim, Seong Keun Kim, Inho Kim, Byung Joon Choi, and Doo Seok Jeong. Leaky integrate-and-fire neuron circuit based on floating-gate integrator. *Frontiers in Neuroscience*, 10, 2016. ISSN 1662-453X. doi: 10.3389/fnins.2016.00212. URL https://www.frontiersin.org/article/10.3389/fnins.2016.00212.

[25] Laura Kriener, Julian Göltz, and Mihai A. Petrovici. The yin-yang dataset, 2022.

[26] Y. Kuroe and H. Iima. A learning method for synthesizing spiking neural oscillators. In *The 2006 IEEE International Joint Conference on Neural Network Proceedings*, pages 3882–3886, 2006. doi: 10.1109/IJCNN.2006.246885.

[27] Yasuaki Kuroe and Tomokazu Ueyama. Learning methods of recurrent spiking neural networks based on adjoint equations approach. In *The 2010 International Joint Conference on Neural Networks (IJCNN)*, pages 1–8, 2010. doi: 10.1109/IJCNN.2010.5596914.

[28] Chankyu Lee, Priyadarshini Panda, Gopalakrishnan Srinivasan, and Kaushik Roy. Training deep spiking convolutional neural networks with stdp-based unsupervised pre-training followed by supervised fine-tuning. *Frontiers in Neuroscience*, 12, 2018. ISSN 1662-453X. doi: 10.3389/fnins.2018.00435. URL https://www.frontiersin.org/article/10.3389/fnins.2018.00435.

[29] Tao Liu, Zihao Liu, Fuhong Lin, Yier Jin, Gang Quan, and Wujie Wen. Mt-spike: A multilayer time-based spiking neuromorphic architecture with temporal error backpropagation. pages 450–457, 11 2017. doi: 10.1109/ICCAD.2017.8203812.

[30] Sergey A. Lobov, Alexey N. Mikhaylov, Maxim Shamshin, Valeri A. Makarov, and Victor B. Kazantsev. Spatial properties of stdp in a self-learning spiking neural network enable controlling a mobile robot. *Frontiers in Neuroscience*, 14, 2020. ISSN 1662-453X. doi: 10.3389/fnins.2020.00088. URL https://www.frontiersin.org/article/10.3389/fnins.2020.00088.

[31] Wolfgang Maass. Networks of spiking neurons: The third generation of neural network models. *Neural Networks*, 10(9):1659–1671, 1997. ISSN 0893-6080. doi: https://doi.org/10.1016/S0893-6080(97)00011-7. URL https://www.sciencedirect.com/science/article/pii/S0893608097000117.

[32] Timoleon Moraitis, Abu Sebastian, and Evangelos Eleftheriou. Optimality of short-term synaptic plasticity in modelling certain dynamic environments, 2020. URL https://arxiv.org/abs/2009.06808.

[33] Hesham Mostafa. Supervised learning based on temporal coding in spiking neural networks. *IEEE Transactions on Neural Networks and Learning Systems*, PP, 06 2016. doi: 10.1109/TNNLS.2017.2726060.

[34] Emre O. Neftci, Hesham Mostafa, and Friedemann Zenke. Surrogate gradient learning in spiking neural networks. *ArXiv*, abs/1901.09948, 2019.

[35] Priyadarshini Panda, Aparna Aketi, and Kaushik Roy. Toward scalable, efficient, and accurate deep spiking neural networks with backward residual connections, stochastic softmax, and hybridization. *Frontiers in Neuroscience*, 14:653, 06 2020. doi: 10.3389/fnins.2020.00653.

[36] Michael Pfeiffer and Thomas Pfeil. Deep learning with spiking neurons: Opportunities and challenges. *Frontiers in Neuroscience*, 12, 2018. ISSN 1662-453X. doi: 10.3389/fnins.2018.00774. URL https://www.frontiersin.org/article/10.3389/fnins.2018.00774.

[37] Kaushik Roy, Akhilesh Jaiswal, and Priyadarshini Panda. Towards spike-based machine intelligence with neuromorphic computing. *Nature*, 575:607–617, 11 2019. doi: 10.1038/s41586-019-1677-2.

[38] Bodo Rueckauer, Iulia-Alexandra Lungu, Yuhuang Hu, Michael Pfeiffer, and Shih-Chii Liu. Conversion of continuous-valued deep networks to efficient event-driven networks for image classification. *Frontiers in Neuroscience*, 11, 2017. ISSN 1662-453X. doi: 10.3389/fnins.2017.00682. URL https://www.frontiersin.org/article/10.3389/fnins.2017.00682.

[39] Berthold Ruf and Michael Schmitt. *Hebbian learning in networks of spiking neurons using temporal coding*, pages 380–389. 04 2006. ISBN 978-3-540-63047-0. doi: 10.1007/BFb0032496.

[40] Ali Safa, Francky Catthoor, and Georges G.E. Gielen. Convsnn: A surrogate gradient spiking neural framework for radar gesture recognition. *Software Impacts*, 10:100131, 2021. ISSN 2665-9638. doi: https://doi.org/10.1016/j.simpa.2021.100131. URL https://www.sciencedirect.com/science/article/pii/S2665963821000531.

[41] Kukan Selvaratnam, Yasuaki Kuroe, and Takehiro Mori. Learning methods of recurrent spiking neural networks. 2000.

[42] Sumit Bam Shrestha and Garrick Orchard. Slayer: Spike layer error reassignment in time. In S. Bengio, H. Wallach, H. Larochelle, K. Grauman, N. Cesa-Bianchi, and R. Garnett, editors, *Advances in Neural Information Processing Systems*, volume 31. Curran Associates, Inc., 2018. URL https://proceedings.neurips.cc/paper/2018/file/82f2b308c3b01637c607ce05f52a2fed-Paper.pdf.

[43] Amirhossein Tavanaei, Masoud Ghodrati, Saeed Reza Kheradpisheh, Timothée Masquelier, and Anthony Maida. Deep learning in spiking neural networks. *Neural Networks*, 04 2018. doi: 10.1016/j.neunet.2018.12.002.

[44] Xiangwen Wang, Xianghong Lin, and Xiaochao Dang. Supervised learning in spiking neural networks: A review of algorithms and evaluations. *Neural Networks*, 125:258–280, 05 2020. doi: 10.1016/j.neunet.2020.02.011.

[45] Timo Wunderlich and Christian Pehle. Event-based backpropagation can compute exact gradients for spiking neural networks. *Scientific Reports*, 11:12829, 06 2021. doi: 10.1038/s41598-021-91786-z.

[46] Friedemann Zenke and Surya Ganguli. SuperSpike: Supervised Learning in Multilayer Spiking Neural Networks. *Neural Computation*, 30(6):1514–1541, 06 2018. ISSN 0899-7667. doi: 10.1162/neco_a_01086. URL https://doi.org/10.1162/neco_a_01086.

[47] Wenrui Zhang and Peng Li. Spike-train level backpropagation for training deep recurrent spiking neural networks. In H. Wallach, H. Larochelle, A. Beygelzimer, F. d'Alché-Buc, E. Fox, and R. Garnett, editors, *Advances in Neural Information Processing Systems*, volume 32. Curran Associates, Inc., 2019. URL https://proceedings.neurips.cc/paper/2019/file/f42a37d114a480b6b57b60ea9a14a9d2-Paper.pdf.

Appendix A. Appendix

A.1. Pre-Synaptic Model

For the ease of presentation, a generic structure of a SNN is illustrated in Fig. 1 on the left. There are many different models to simulate the nonlinear dynamics of a spiking neuron (e.g., see [16]). In this paper, we adopt the Leaky-Integrate-and-Fire (LIF) model which consists of three main steps.
(i) Synaptic Dynamics. A generic neuron i is stimulated through a collection of input neurons, its neighborhood $\mathcal{N}_i$. Each neuron $j \in \mathcal{N}_i$ has a synaptic connection to i whose dynamics is modelled by a 1st-order low-pass RC circuit that smooths out the Dirac Delta currents it receives from neuron j. Since this system is linear and time-invariant (LTI), it can be described by its impulse response

$$h_j^s(t) = e^{-\alpha_j t} u(t),$$

where $\alpha_j = \frac{1}{\tau_j^s}$ and $\tau_j^s = R_j^s C_j^s$ denotes the synaptic time constant of neuron j, and $u(t)$ denotes the Heaviside step function. Therefore, the output synaptic current $I_j(t)$ can be written as

$$I_j(t) = h_j^s(t) \star \sum_{f \in \mathcal{F}_j} \delta(t-f) = \sum_{f \in \mathcal{F}_j} h_j^s(t-f), \tag{7}$$

where $\mathcal{F}_j$ is the set of output firing times from neuron j. Note that in Eq. (7) we used the fact that convolution with a Direct Delta function $h_j^s(t) \star \delta(t-f) = h_j^s(t-f)$, is equivalent to shifts in time.
(ii) Neuron Dynamics. The synaptic current of all stimulating neurons is weighted by W_{ji}, $j \in \mathcal{N}_i$, and builds the weighted current that feeds the neuron. The dynamic of the neuron can be described by yet another 1st-order low-pass RC circuit with a time constant $\tau_i^n = R_i^n C_i^n$ and with an impulse response $h_i^n(t) = e^{-\beta_i t} u(t)$ where $\beta_i = \frac{1}{\tau_i^n}$. The output of this system is the potential $V_i(t)$.
(iii) Hard-thresholding and spike generation. The membrane potential $V_i(t)$ is compared with the firing threshold θ_i of neuron i and a spike (a Delta current) is produced by neuron when $V_i(t)$ goes above θ_i. Also, after spike generation, the membrane potential is reset/dropped immediately by θ_i.

A.2. Proof of Theorem 3

Proof In the following, we provide a a simple and intuitive proof. An alternative and more rigorous proof by induction on the number of firing times of neuron i is provided in Appendix A.3.
Proof (i): We use the following simple result/computation-trick from circuit theory that in an RC circuit, abrupt dropping of the potential of the capacitor by θ_i at a specific firing time $f \in \mathcal{F}_i$ can be mimicked by adding a voltage source $-\theta_i u(t-f)$ series with the capacitor. If we do this for all the firing times of the neuron, we obtain a linear RC circuit with two inputs: (i) weighted synaptic current coming from the neurons $\mathcal{N}_i$, (ii) voltage sources $\{-\theta_i u(t-f) : f \in \mathcal{F}_i\}$. See Fig. 2 (left).

The key observation is that although this new circuit is obtained after running the dynamics of the neuron and observing its firing times $\mathcal{F}_i$, as far as the membrane potential $V_i(t)$ is concerned, the two circuits are equivalent. Interestingly, after this modification, the new circuit is a completely linear circuit and we can apply the super-position principle for linear circuits to write the response of the neuron as the summation of: (i) the response $V_i^{(1)}(t)$ due to the weighted synaptic current $I_i^s(t)$ in the input (as in the previous circuit), and (ii) the response $V_i^{(2)}(t)$ due to Heaviside voltage sources $\{-\theta_i u(t-f) : f \in \mathcal{F}_i\}$. From (2), $V_i^{(1)}(t)$ is simply given by $V_i^{(1)}(t) = \sum_{j \in \mathcal{N}_i} W_{ji} y_{ji}(t)$.

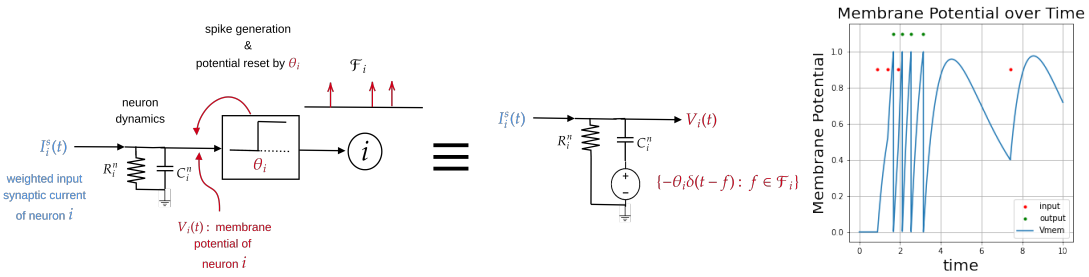

Figure 2: **(Left)** Equivalence of response for: (i) a nonlinear neuron with weighted synaptic currents $I(t)$ and spike generation, and (ii) a linear neuron with input $I(t)$ and Heaviside voltages $\{-\theta_i u(t-f) : f \in \mathcal{F}_i\}$. **(Right)** Plot of membrane potential over time using Eq. (8).

The response of an RC circuit to a Heaviside voltage function $-\theta_i u(t-f)$ is given by $-\theta_i h_i^n(t-f)$ where $h_i^n(t)$ is the impulse response of the neuron i as before. We also used the time invariance property (for shift by f) and a well-known result from circuit theory (Thevenin-Norton theorem) that for an RC circuit the impulse response due to a Delta current source is the same as the impulse response due to a Heaviside voltage source. The response to all Heaviside voltage functions, from super-position principle, is simply given by $V_i^{(2)}(t) = -\theta_i \sum_{f\in\mathcal{F}_i} h_i^n(t-f)$. Therefore, we obtain that

$$V_i(t) = V_i^{(1)}(t) + V_i^{(2)}(t) = \sum_{j\in\mathcal{N}_i} W_{ji} y_{ji}(t) - \sum_{f\in\mathcal{F}_i} \theta_i h_i^n(t-f). \tag{8}$$

This completes the proof. See Fig. 2 (right). ■

A.3. Alternative Proof of Theorem 3

Proof (ii): Here we provide a more rigorous proof based on induction on the number of firing times $\mathsf{F}_i := |\mathcal{F}_i|$ of the neuron i.

We first check the base of the induction. If there are no firing times, i.e., $\mathcal{F}_i = \emptyset$ and $F_i = 0$, then there is no source of non-linearity and the neuron is a fully linear system. Thus, the response of the neuron to the input weighted synaptic current $I_i^s(t)$ is given, as in (2), by

$$V_i(t) = \sum_{j\in\mathcal{N}_i} W_{ji} y_{ji}(t),$$

which yields the desired result since, for $\mathcal{F}_i = \emptyset$, the second term $-\sum_{f\in\mathcal{F}_i} \theta_i h_i^n(t-f)$ is zero. This confirms the base of induction for $\mathsf{F}_i = 0$.

Now let us assume that $\mathcal{F}_i \neq \emptyset$ and the neuron i has fired at least once ($\mathsf{F}_i \geq 1$). Here, we can still check that result holds for all time $t \in [0, f_1)$ before the first firing time f_1 because before the first firing time the circuit is completely linear (thus, the first term) and the second term is equal to zero as $h_i^n(t-f_1) = e^{\beta_i(t-f_1)} u(t-f_1)$ is equal to zero for all $t < f_1$ (due to causality and the fact that $u(t-f_1) = 0$ for $t < f_1$).

Now we prove that if the result is true for $t \in [0, f^k)$ it remains true for $t \in [f_k, f_{k+1})$ where we denote the k-th and $(k+1)$-th firing times by f_k and f_{k+1} and apply the convention that $f_k = \infty$ for $k > F_i$.

To prove this, we first note that the weighted synaptic current (see, e.g., Fig. 2) coming from the neurons $\mathcal{N}_i$ is given by

$$I_i^s(t) = \sum_{j \in \mathcal{N}_i} W_{ji} \sum_{g \in \mathcal{F}_i} h_j^s(t-g)$$

for all times $t \geq 0$. Also, note that since synapses are always linear, this is true independent of whether there is any firing and potential drop at the neuron i. At the firing time f_k the value of potential drops to $V_i^{(k)} = V_i(f_k) - \theta_i$. Thus, to prove the result, we need to find and verify the response of the neuron to the synaptic current $I_i^s(t)$ for $t \in [f_k, f_{k+1})$ starting from the initial value $V_i^{(k)}$. Here again we note that starting from f_k the system is again linear until the next firing time f_{k+1}. Thus, we can again apply the super position principle for linear systems to decompose the response into two parts: (a) response to the initial condition $V_i^{(k)}$ and (b) response to the input synaptic current $I_i^s(t)$.

From the linearity and time-invariance of RC circuits, (a) is simply given by

$$\begin{aligned} V_i^{(a)}(t) &= V_i^{(k)} h_i^n(t-f_k) \\ &= V_i^{(k)} e^{-\beta_i(t-f_k)} u(t-f_k) \\ &= V_i(f_k) e^{-\beta_i(t-f_k)} u(t-f_k) - \theta_i h_i^n(t-f_k), \end{aligned}$$

where $h_i^n(t) = e^{-\beta_i t} u(t)$ is the impulse response of the neuron i.

The response to the synaptic current in the time interval $t \in [f_k, f_{k+1})$ is also given by

$$\begin{aligned} V_i^{(b)}(t) &\overset{(i)}{=} I_i^s(t) u(t-f_k) \star h_i^n(t) \\ &= \int_0^\infty I_i^s(\lambda) u(\lambda - f_k) h_i^n(t-\lambda) d\lambda \\ &\overset{(ii)}{=} \int_{f_k}^t I_i^s(\lambda) h_i^n(t-\lambda) d\lambda \\ &= \int_0^t I_i^s(\lambda) h_i^n(t-\lambda) d\lambda - \int_0^{f_k} I_i^s(\lambda) h_i^n(t-\lambda) d\lambda \\ &= I_i^s(t) \star h_i^n(t) - \int_0^{f_k} I_i^s(\lambda) e^{-\beta_i(t-\lambda)} d\lambda \\ &= I_i^s(t) \star h_i^n(t) - e^{-\beta_i(t-f_k)} \int_0^{f_k} I_i^s(\lambda) e^{-\beta_i(f_k-\lambda)} d\lambda \\ &= I_i^s(t) \star h_i^n(t) - I_i^s(t) \star h_i^n(t)\Big|_{t=f_k} \times e^{-\beta_i(t-f_k)}, \end{aligned}$$

where in (i) we multiplied $I_i^s(t)$ with $u(t-f_k)$ to remove the effect of the synaptic current before f_k (since, due to causality, it cannot affect the neuron potential in the time interval $t \in [f_k, f_{k+1})$), where in (ii) we used the fact that, due to causality, $h_{ni}(t-\lambda) = 0$ for $\lambda > t$, and that $u(\lambda - f_k)$ is zero for $\lambda < f_k$.

From the induction hypothesis applied to $f_k \in [0, f_k]$, we have that

$$\begin{aligned}
V_i(f_k) &= I_i^s(t) \star h_i^n(t)\Big|_{t=f_k} - \theta_i \sum_{l=1}^{k-1} h_i^n(f_k - f_l) \\
&= I_i^s(t) \star h_i^n(t)\Big|_{t=f_k} - \theta_i \sum_{l=1}^{k-1} h_i^n(f_k - f_l) \\
&= I_i^s(t) \star h_i^n(t)\Big|_{t=f_k} - \theta_i \sum_{l=1}^{k-1} e^{-\beta_i(f_k - f_l)} \\
&= I_i^s(t) \star h_i^n(t)\Big|_{t=f_k} - \theta_i e^{\beta_i(t-f_k)} \sum_{l=1}^{k-1} e^{-\beta_i(t-f_l)} \\
&= I_i^s(t) \star h_i^n(t)\Big|_{t=f_k} - \theta_i e^{\beta_i(t-f_k)} \sum_{l=1}^{k-1} h_i^n(t - f_l).
\end{aligned}$$

Therefore, after simplification, we obtain that

$$I_i^s(t) \star h_i^n(t)\Big|_{t=f_k} \times e^{-\beta_i(t-f_k)} \tag{9}$$

$$= V_i(f_k) e^{-\beta_i(t-f_k)} + \theta_i \sum_{l=1}^{k-1} h_i^n(t - f_l). \tag{10}$$

Replacing in (9), therefore, we obtain

$$V_i^{(b)}(t) = I_i^s(t) \star h_i^n(t) \tag{11}$$

$$- V_i(f_k) e^{-\beta_i(t-f_k)} - \theta_i \sum_{l=1}^{k-1} h_i^n(t - f_l). \tag{12}$$

Applying the super position principle, we have

$$\begin{aligned}
V_i(t) &= V_i^{(a)}(t) + V_i^{(b)}(t) \\
&= I_i^s(t) \star h_i^n(t) - \theta_i \sum_{l=1}^{k-1} h_i^n(t - f_l) - \theta_i h_i^n(t - f_k) \\
&= I_i^s(t) \star h_i^n(t) - \theta_i \sum_{l=1}^{k} h_i^n(t - f_l) \\
&= \Big(\sum_{j \in \mathcal{N}_i} W_{ji} \sum_{g \in \mathcal{F}_i} h_j^s(t - g) \Big) \star h_i^n(t) - \theta_i \sum_{l=1}^{k} h_i^n(t - f_l) \\
&= \sum_{j \in \mathcal{N}_i} W_{ji} \sum_{g \in \mathcal{F}_i} h_{ji}(t - g) - \theta_i \sum_{l=1}^{k} h_i^n(t - f_l) \\
&= \sum_{j \in \mathcal{N}_i} W_{ji} y_{ji}(t) - \theta_i \sum_{f \in \mathcal{F}_i} h_i^n(t - f),
\end{aligned}$$

where in the last equation we used the fact that $h_i^n(t-f)=0$ for $t \in [f_k, f_{k+1})$ and for $f > f_{k+1}$. This validates the result for $t \in [f_k, f_{k+1})$, and verifies the induction. This completes the proof.

A.4. Implicit Function Theorem

In many problem in machine learning, statistics, control theory, mathematics, etc. we use a collection of variables to track/specify the state of an algorithm, a dynamical system, etc. However, in practice, these variables are not completely free and are connected to each other via specific constraints. In such cases, we are always interested to know the functional relation between these variables, namely, how changing some variables affect the others (sensitivity analysis). IFT theorem provides a rigorous method for these types of analyses when the variables are connected through differentiable equality constraints, as illustrated in the following theorem.

Theorem 10 (Implicit Function Theorem) *Let $\phi : \mathbb{R}^n \times \mathbb{R}^m \to \mathbb{R}^m$ be a differentiable function and let $\mathcal{Z} = \{(x, y) \in \mathbb{R}^n \times \mathbb{R}^m : \phi(x, y) = 0\}$ be the zero-set of ϕ. Suppose that $\mathcal{Z} \neq \emptyset$ and let $(x_0, y_0) \in \mathcal{Z}$ be an arbitrary point. Also, let $\frac{\partial \phi}{\partial y}\phi(x_0, y_0)$ be the $m \times m$ matrix of partial derivatives w.r.t. y and assume that it is non-singular, i.e., $det\big(\frac{\partial \phi}{\partial y}(x_0, y_0)\big) \neq 0$. Then,*

- *There is an open neighborhood $\mathcal{N}_x$ around x_0 and an open neighborhood $\mathcal{N}_y$ around y_0 such that $\frac{\partial \phi}{\partial y}\phi(x, y)$ is non-singular for all $(x, y) \in \mathcal{N} := \mathcal{N}_x \times \mathcal{N}_y$ (including of course the original (x_0, y_0)).*
- *There is a function $\psi : \mathcal{N}_x \to \mathcal{N}_y$ such that $(x, \psi(x))$ belongs to the zero set $\mathcal{Z}$, namely, $\phi(x, \psi(x)) = 0$, for all $x \in \mathcal{N}_x$; therefore, the variables y in $\mathcal{N}_y$ can be written as a function $y = \psi(x)$ of the variables x in $\mathcal{N}_x$.*
- *ψ is a differentiable function of x for $x \in \mathcal{N}_x$ and*

$$\frac{\partial \phi}{\partial y} \times \frac{\partial \psi}{\partial x} + \frac{\partial \phi}{\partial x} = 0, \tag{13}$$

which from the non-singularity of $\frac{\partial \phi}{\partial y}$ yields

$$\frac{\partial \psi}{\partial x} = -\Big(\frac{\partial \phi}{\partial y}\Big)^{-1} \times \frac{\partial \phi}{\partial x}. \tag{14}$$

Example 1. Fig. 3 illustrates the zero-set $\mathcal{Z} = \{(x, y) : \phi(x, y) = 0\}$ of a function $\phi : \mathbb{R}^2 \to \mathbb{R}$. To investigate the conditions of the implicit function theorem, we first note that the gradient of ϕ denoted by $\nabla\phi = (\frac{\partial \phi}{\partial x}, \frac{\partial \phi}{\partial y})$ is always orthogonal to the level-set (here the zero-set) of ϕ. Thus, by observing the orthogonal vector to curve, we can verify if $\frac{\partial \phi}{\partial x}$ or $\frac{\partial \phi}{\partial y}$ are non-singular (non-zero in the scalar case we consider here). We investigate several cases:

- Point C: gradient vector does not exist, so the assumptions of the IFT are not fulfilled. One can also see that at C one cannot write neither x as a function of y nor y as a function of x.
- Point A: gradient vector has zero horizontal and non-zero vertical component , i.e., $\frac{\partial \phi}{\partial x} = 0$ and $\frac{\partial \phi}{\partial y} \neq 0$. Thus, from IFT, in a local neighborhood of A, one should be able to write only y as a differentiable function of x.

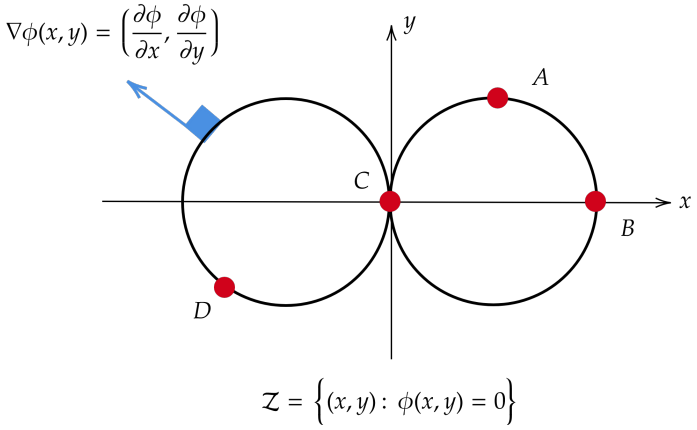

Figure 3: Illustration of the implicit function theorem.

- Point B: gradient has zero horizontal component. And, only x can be written as differentiable function of y.
- Point D: gradient has non-zero horizontal and vertical components. So, in a local neighborhood of D, one may write both x and y as a differentiable function of the another.

A.5. Proof of Theorem 4

Proof (i) Note that in our post-synaptic kernel model derived in Section 2.1, the membrane potential of the output layer $V_o(t)$ can be written (in a more expanded form) as

$$V_o(t) = \sum_{j\in\mathcal{N}_o} W_{jo} \sum_{g\in\mathcal{F}_j} h_{jo}(t-g). \tag{15}$$

Note that we dropped the term $-\theta_o \sum_{f\in\mathcal{F}_o} h_o^n(t-f)$ due to potential reset because we always assume that the output neuron is linear in regression tasks where $V_o(t)$ appears directly in the loss. It is also seen that $V_o(t)$ at each time t is a function of all the firing times $\mathcal{F}$ and also weights W.

(ii) Since $\ell_{\mathcal{F}}$ is assumed to be a differentiable function of $\mathcal{F}$ and W, we need to verify only the differentiability of the integral expression in (4). First note that $h_{jo}(t)$ is a differentiable function except at $t=0$ where, albeit being non-differentiable, it has finite left and right derivatives. This implies that $V_o(t)$ in (15) is differentiable at all t except at the firing times of its stimulating neuron $\mathcal{N}_o$, where at those points it has finite left and right derivatives. Therefore, we may write

$$\frac{\partial}{\partial\mathcal{F}} \int_0^T \ell_V(V_o(t),\mathcal{F};W)\mathrm{dt} = \int_0^T \frac{\partial\ell_V}{\partial V_o}(V_o(t),\mathcal{F};W)\frac{\partial V_o(t)}{\partial\mathcal{F}} + \int_0^T \frac{\partial\ell_V}{\partial\mathcal{F}}(V_o(t),\mathcal{F};W)\mathrm{dt}.$$

Since ℓ_V is assumed to be a differentiable function of $\mathcal{F}$, the second integral is well-defined. Also, ℓ_V is differentiable w.r.t. V_o. And $V_o(t)$, being a weighted combination of terms $h_{ji}(t-g)$ with $g \in \sqcup_{j\in\mathcal{N}_o}\mathcal{F}_j$, is a differentiable function of firing times $\mathcal{F}$ except perhaps at finitely many points $t \in \sqcup_{j\in\mathcal{N}_o}\mathcal{F}_j$ where at those points it may be discontinuous but has finite left and right derivatives. This implies that the first integral is also well-defined.

(iii) Since from (ii), the loss $\mathcal{L} = \mathcal{L}(\mathcal{F}; W)$ is a differentiable function of both $\mathcal{F}$ and W, we have that

$$\frac{\partial \mathcal{L}}{\partial W} = \mathcal{L}_1 \frac{\partial \mathcal{F}}{\partial W} + \mathcal{L}_2 \tag{16}$$

where $\mathcal{L}_1$ and $\mathcal{L}_2$ denote the partial derivative of $\mathcal{L}$ w.r.t. its 1st and 2nd argument, and where we used the fact that from (ii) both $\mathcal{L}_1$ and $\mathcal{L}_2$ are well-defined. It is seen that the gradients of loss w.r.t. W exist provided that the firing times $\mathcal{F}$ are differentiable w.r.t. the weights. This completes the proof. ■

A.6. Example: Causality and Differentiability

In order to track the effects of previous layers' firing times on a current neuron i, we can map which firing times of a previous neuron directly cause the firing of a neuron that it feeds into, and so on through the network. Consider the following simple example of a simple 3 neuron feed-forward network with 1 input dimension:

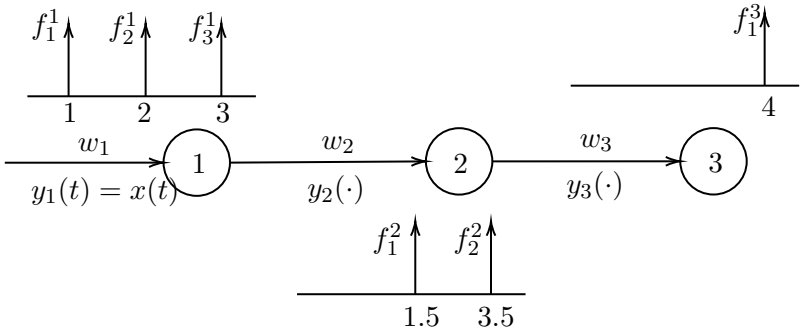

For simplicity, we will assume all neurons have the same parameters α, β, θ. Let w_1, w_2, w_3 be the weights corresponding to the inputs to neurons 1, 2, and 3, respectively. Suppose that neuron 1 had firing times at $f_1^1 = 1, f_2^1 = 2$, and $f_3^1 = 3$. Neuron 2 fired at $f_1^2 = 1.5$ and $f_2^2 = 3.5$. Finally neuron 3 fired at $f_1^3 = 4$. Note that the only firing times that could cause neuron 2 to fire at $f_1^2 = 1.5$ had to occur before $t = 1.5$. This is only $f_1^1 = 1$. Once neuron 2 fires at f_1^2, its potential is reset, so then the next time it fires at f_2^2 it is only affected by f_2^1 and f_3^2. Similarly, $f_2^2 = 3.5$ is affected by f_3^2. And similarly, f_1^2 and f_2^2 affects f_1^3. This corresponds to the following causality diagram:

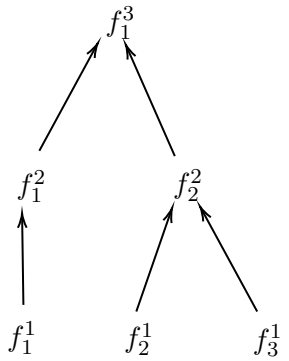

Note that while this simple example is for the reset to zero regime, where the membrane potential resets completely to 0 and all inputs in-between firing times accumulate until the next time the neuron fires, this kind of diagram can similarly be constructed for other regimes. For instance, if there is a time delay before inputs can start increasing the membrane potentials again, to decide the causal edges for a current firing time for a neuron we would have to look for input firing times that occurred at least "time delay" seconds after the current neuron's previous firing time.

We will use equations (1), (3), and (8) to define the following system. Since all neurons share the same parameters α, β, we can simplify some notation and refer to the joint impulse response coming into a neuron as h_{s+n} which corresponds to equation (1) and the impulse response for just the membrane potential dynamics as h_n which corresponds to the h_i^n term in equation (3).

$$
\begin{aligned}
w_1 \cdot \sum_{t:x(t)=1 \wedge t<f_1^1} h_{s+n}(f_1^1 - t) &= \theta && \text{Eq. for } f_1^1 \\
w_1 \cdot \sum_{t:x(t)=1 \wedge f_1^1<t<f_2^1} h_{s+n}(f_2^1 - t) - \theta \cdot h_n(f_2^1 - f_1^1) &= \theta && \text{Eq. for } f_2^1 \\
w_1 \cdot \sum_{t:x(t)=1 \wedge f_2^1<t<f_3^1} h_{s+n}(f_3^1 - t) - \theta \cdot \big(h_n(f_3^1 - f_1^1) + h_n(f_3^1 - f_2^1)\big) &= \theta && \text{Eq. for } f_3^1 \\
w_2 \cdot h_{s+n}(f_1^2 - f_1^1) &= \theta && \text{Eq. for } f_1^2 \\
w_2 \cdot \big(h_{s+n}(f_2^2 - f_2^1) + h_{s+n}(f_2^2 - f_3^1)\big) - \theta \cdot h_n(f_2^2 - f_1^2) &= \theta && \text{Eq. for } f_2^2 \\
w_3 \cdot \big(h_{s+n}(f_1^3 - f_1^2) + h_{s+n}(f_1^3 - f_2^2)\big) &= \theta && \text{Eq. for } f_1^3
\end{aligned}
$$

Now, all 6 equations are equations of the network weights (w_1, w_2, w_3) and the 6 firing times $(f_1^1, f_2^1, f_3^1, f_1^2, f_2^2, f_1^3)$. Here, we invoke the implicit function theorem which will allow us to express firing times as a function of the weights.

We just need to check that the Jacobian of the above 6 equations (treated as a vector valued function) differentiated w.r.t. the 6 firing times is invertible. It turns out the causality structure will ensure that the Jacobian is always lower triangular once you sort by firing times. For feed-forward networks, this is also true if you sort by firing times by layer (since firing times within the same layer do not affect each other, and the firing times of deeper layers do not affect earlier ones). This Jacobian look like

$$
\begin{array}{l}
 \\
V_1(f_1^1) - \theta = 0 \\
V_1(f_2^1) - \theta = 0 \\
V_1(f_3^1) - \theta = 0 \\
V_2(f_1^2) - \theta = 0 \\
V_2(f_2^2) - \theta = 0 \\
V_3(f_1^3) - \theta = 0
\end{array}
\begin{array}{c}
\begin{array}{cccccc} f_1^1 & f_2^1 & f_3^1 & f_1^2 & f_2^2 & f_1^3 \end{array} \\
\begin{pmatrix}
x & & & & & \\
x & x & & & & \\
x & x & x & & & \\
x & & & x & & \\
 & x & x & x & x & \\
 & & & x & x & x
\end{pmatrix}
\end{array}
$$

where x is marked for each equation there is a nontrivial derivative w.r.t. the corresponding variable. The lower triangular structure occurs because of the way later firing times cannot occur in the equations for earlier ones.

Invertibility holds as long as the diagonal elements are non-zero. Since each equation is equal to the membrane potential at the firing threshold, the derivative of the membrane potential w.r.t. its firing time is the equal to the derivative of the membrane potential w.r.t. t evaluated at the firing time, which is strictly positive because the potential is increasing at firing time.

A.7. Algorithm Details

A.7.1. CAUSALITY GRAPH

Due to the formula in Eq. (3), calculating the membrane potential at any given time just relies on keeping track of which firing times from the previous (feeding) neuron(s) caused the current one to spike. Thus to efficiently calculate partial derivatives, we will keep track of this information while calculating network firing outputs. A detailed explanation on a small example is given in A.6.

A.7.2. FORWARD SPIKE TIME COMPUTATION

Simulating an SNN in the forward pass and computing the firing times of its neurons requires solving the Euler integration corresponding to the differential equation of the synapse and membrane potentials. This is usually done approximately by quantizing time into small steps and iteratively updating potentials. There are several libraries such as snnTorch [13] that implement this. Our method for gradient computation can definitely use these methods in its forward pass where the firing times are computed.

Here, however, we propose another method that uses the impulse response (kernel) representation of the corresponding differential equations derived in (1) and (3) to compute the firing times exactly without any need for time quantization. The main idea behind this method is that for exponential synaptic and membrane impulse responses, one can always write the membrane potential of a neuron over a time interval $[t_0, t_1]$ at which the neuron receives no spikes at its input as $Ae^{-\alpha t} + Be^{-\beta t}$ where A and B are some suitable coefficients and where α, β are the inverse synaptic and membrane time constants (common to all neurons), respectively. [1] Thus the next firing time can be found by computing the time t, in case there is any, at which this curve intersects the horizontal line θ. Once this firing time is computed, we update the coefficients A and B and the search interval $[t_0, t_1]$ depending on whether the neuron receives any spikes before this firing time, and continue this until all the firing times are computed. This is summarzied in Algorithm 1.

Remark 11 *Note that one can calculate partial derivatives of each firing time equation w.r.t. input firing times, the neuron's previous firing times, and the input weights after solving for the firing time and computing the causality graph. In feed-forward networks, these calculations for neurons in the same layer can be parallelized since the firing times of neurons in the same layer will not affect each other.*

1. For example, consider only two input spikes at times t_1 and $t_2 > t_1$ with associated weights W_{1i} and W_{2i}. Then the total kernel value at $t \in [t_2, \infty)$ (at which there are no other input spikes) is given by $W_{1i}h_{1i}(t - t_1) + W_{2i}h_{2i}(t - t_2) = \frac{W_{1i}e^{\beta t_1} + W_{2i}e^{\beta t_2}}{\alpha - \beta} e^{-\beta t} + \frac{W_{1i}e^{\alpha t_1} + W_{2i}e^{\alpha t_2}}{\beta - \alpha} e^{-\alpha t}$. In case the neuron fires, e.g., at time t_f, we need to account for the potential resets by subtracting the term $\theta e^{-\beta(t-t_f)}u(t-t_f)$, which is again in the exponential form $\theta e^{\beta t_f} \times e^{-\beta t}$ for $t > t_f$. Thus the whole expression, for $t > t_2$ and before the next firing time, can be written as $Ae^{-\alpha t} + Be^{-\beta t}$.

Algorithm 1 Firing Time Computation

Input: Firing times $\mathcal{F} = \sqcup_j \mathcal{F}_j$ from neighbors $j \in \mathcal{N}_i$ and weights W_{ji}.
Hyperparameters α, β, θ_i.
Initialize $A, B = 0$.
Initialize empty queue.
for f (sorted) **in** $\mathcal{F}$ **do**

- Append f to queue.
- Solve for t:

$$Ae^{-\alpha t} + Be^{-\beta t} = \theta_i.$$

- Append t to output.
- Update A and B.
- Add entire queue as causal edges to t.
- (Empty queue if no synaptic dynamics.)

end for
Return Causal graph and firing times.

Algorithm 2 Forward Propagation

Input: Network output firing times $\mathcal{F} = \sqcup_i \mathcal{F}_i$ for all i and causal graph (e.g., by Alg. 1).
Initialize matrices $\mathbf{L}$, $\frac{\partial \mathcal{F}}{\partial W}$, and $\frac{\partial \mathbb{V}}{\partial W}$.
for f (sorted) **in** $\mathcal{F}$ **do**
Calculate partial derivatives of the firing time equation for f output by neuron i: $V_i(f) - \theta_i = 0$.

- Use causal information and Eq. (3) to fully describe $V_i(f)$.
- **Update L.** Calculate $\frac{\partial}{\partial f_{j\to i}}(V_i(f) - \theta_i)$ for each $f_{j\to i}$ in the causal graph for f.
- **Update L.** Calculate $\frac{\partial}{\partial f}(V_i(f) - \theta_i)$.
- **Update $\frac{\partial \mathbb{V}}{\partial W}$.** Calculate $\frac{\partial}{\partial W_{ji}}(V_i(f) - \theta_i)$ for all weights W_{ji} attached to neuron i.
- **IFT Step.** Solve Eq. (6) via back substitution to update $\frac{\partial \mathcal{F}}{\partial W}$.

end for
Calculate $\frac{\partial \mathcal{L}}{\partial W}$ using final $\frac{\partial \mathcal{F}}{\partial W}$ via Eq. (16).

A.7.3. FORWARD PROPAGATION FOR GRADIENT COMPUTATION

The forward propagation algorithm emerges from the earlier presented theorems and observations. We can derive partial derivatives of the total loss by calculating the partial derivatives of the network firing times w.r.t. network weights, which are in turn calculated by applying the implicit function theorem with appropriate partial derivatives of the equations that describe the membrane potentials at each firing time.

Again, due to the lower triangular structure of matrix $\mathbf{L}$ (see, e.g., Theorem 5), we can iteratively solve the linear system (6) of IFT equations without having to do a full matrix inversion. As mentioned earlier, the partial derivatives we need to calculate for the update steps in Algorithm 2 can actually all be done in the forward pass. For feed-forward networks in particular, these can be calculated in the forward pass in parallel within each layer. This incurs a cost of $O(|\mathcal{F}|^2|\mathcal{W}|)$ in time, using $(1 + 2 + 3 + ... + |\mathcal{F}|) \times (\text{ up to } |\mathcal{W}|)$ operations to solve for the $|\mathcal{F}| \times |\mathcal{W}|$ Jacobian matrix. The memory cost is $O(|\mathcal{F}||\mathcal{W}|)$ to store the solutions and one of the Jacobians, where $O(|\mathcal{F}||\mathcal{W}|)$ is always needed for storing the gradients.

A.8. Experiment details

A.8.1. XOR TASK

To investigate whether the network can robustly learn to solve the XOR task as in [33], we reproduced most of the experiment settings in [33] by coding each of the input spikes as 0.0 (early spike)

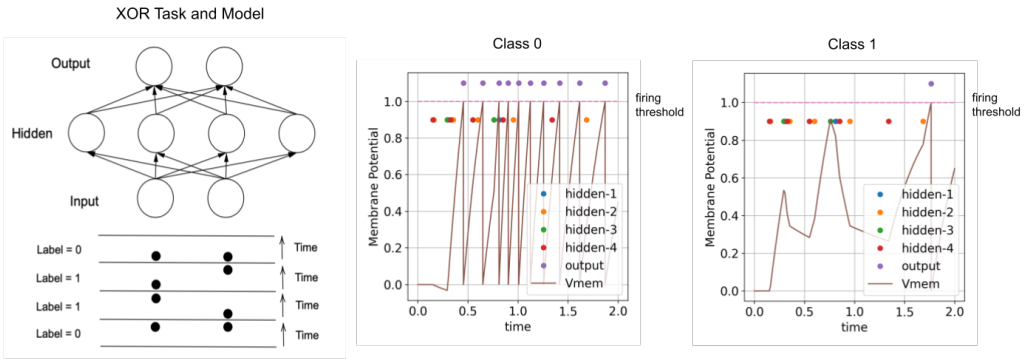

Figure 4: **(Left)** Model for XOR task. **(Right)** Given the input $(0, 0)$, output neurons have different voltage traces. Note that each output neuron has the same input firing times, from each of the 4 hidden layer neurons, but the network is able to learn weights that push the output neuron corresponding to label '1' to spike later, and the one corresponding to label '0' (true label) to spike earlier.

or 2.0 (late spike), which feed into 4 hidden neurons, which in turn feed into 2 output neurons. We use a cross-entropy loss based on first spike times of the output neurons (so the label neuron should fire sooner than the other). For each of 1000 different random weight initializations, we trained until convergence with learning rate 0.1. Unlike in [33], we consider one iteration of training to be just 1 full batch, rather than 100. Across all 1000 trials, the maximum steps to converge was 98, with the average being 17.52 steps. Compare this to maximum 61 training iterations (each iteration seeing 100 full batches of the four input patterns), with average 3.48 iterations in [33]. Figure 4 illustrates the model implementing the XOR task, as well as a post-training simulation of the output neurons' membrane potentials for input $(0, 0)$. No special tuning of hyperparameters of the 2-4-2 network was used, and the network reliably converged to 100% accuracy given the following parameters in Table 1.

A.8.2. IRIS DATASET

We also trained SNN using FP on the Iris dataset to demonstrate learning from data with real-valued features. Note one class is linearly separable from the other 2; the latter are not linearly separable from each other [2, 15]. We encoded the input features with a scheme similar to [29], but modified to where each real-valued feature n_i is transformed into a firing time via the transformation $T \cdot (1 - \frac{n_i - \min(n_i)}{\max(n_i) - \max(n_i)})$, where T is the maximum time horizon and the min/max of a feature is taken over the whole dataset. After training a small 4-10-3 network, we achieve 100% test accuracy (compare to 93.3% for MT-1 (4-25-1) and 96.7% for an MLP ANN (4-25-3) in [29]). Again, the network is able to learn weights to push the true label output neurons to fire earlier than the others, since our loss function is minimized when all the correct label neurons fire before other output neurons. An illustration of this effect is shown in Figure 5. We did a systemic grid search over hyperparameters to find a network suitable for the Iris classification. There were several networks which achieved 100% test accuracy. One such set of hyperparameters is given in Table 2.

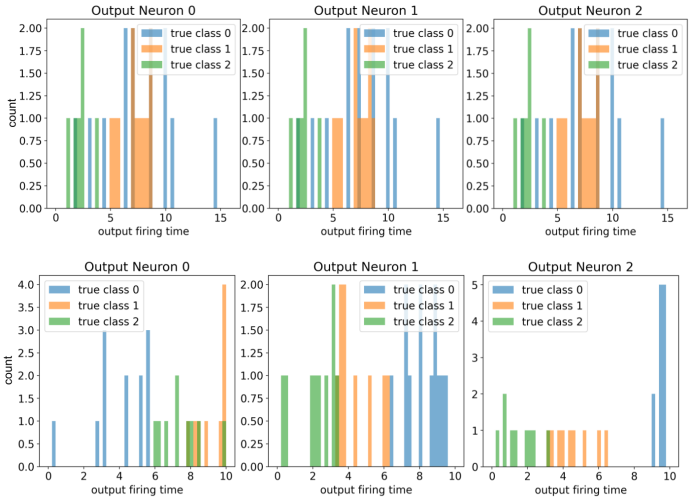

Figure 5: A histogram of the first output firing times of each label neuron, given unseen test data. **(Top)** At random initialization, firing times look the same across all label neurons. **(Bottom)** After training, the firing times are clearly separated into the 3 classes, and all test examples belonging to the same class as the corresponding label neuron fires earlier than in the other label neurons.

A.8.3. YIN-YANG DATASET

We also implemented FP to train SNN on the Yin-Yang dataset which is a two-dimensional and non-linearly separable dataset [25]. The Yin-Yang dataset requires a multi-layer model, as a shallow classifier achieves around 64% accuracy, thus it requires a hidden layer and backpropagation (or forward-propagation in our case) for gradient-based learning to achieve higher accuracy, as noted also in [45].

We used a loss based on the earliest spike times of the 3 output neurons, as in [18, 45] defined as

$$\mathcal{L} = -\frac{1}{N_{\text{batch}}}\left[\sum_{i=1}^{N_{\text{batch}}} \log\left(\frac{e^{-f_{i,l(i)}/\tau_0}}{\sum_{j=1}^{3} e^{-f_{i,j}/\tau_0}}\right) + \gamma\left(e^{f_{i,l(i)}/\tau_1} - 1\right)\right],$$

where $f_{i,j}$ is the first spike time of neuron j for the i^{th} example and $l(i)$ is the index of the correct label for the i^{th} example. The second term is a regularization term which encourages earlier spike times for the true label neuron, its influence on the total loss controlled by γ.

Comparing to surrogate methods. First, to compare training with surrogate gradient methods, we used the snnTorch library [13] to train equivalent models[2], using the same hyperparameters and

2. Many surrogate methods are usually not compatible with training using temporal losses, as noted also by [13] that often the first spike time is non-differentiable with respect to the spikes themselves. To fairly compare to surrogate

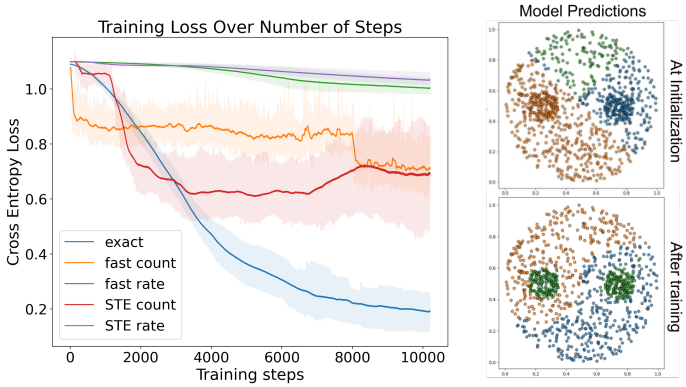

Figure 6: **(Left)** Comparison to surrogate gradients. The plot shows the change in training loss over time for training SNN with exact and surrogate gradients, the fast sigmoid function and straight-through estimator each with a count-based and spike-rate cross entropy loss. **(Right)** A comparison of model predictions at random initialization, versus after training.

initializations, but with surrogate gradients. Fig. 6 (left) compares training with exact gradient (our method) with using the fast sigmoid [46] surrogate function and the straight-through estimator [4], with both count-based cross entropy loss and a spike rate cross entropy loss. (See footnote.) All models at initialization have around 30-36% accuracy and cross entropy loss around 1.09-1.1, but at the end of 300 epochs of training, using exact gradients results in faster loss reduction (as one might expect).

Evaluation. After repeating the experiment with 10 random initializations, a 2-layer SNN model trained with FP obtains a test accuracy with mean **95.0**(0.83)%, comparable to [18] reporting 95.9(0.7)%. It is worth noting that training only involved using the exact gradients for SGD, without employing other heuristics in [18], which include a flat weight bump (increase weights a fixed amount) whenever the proportion of non-spiking neurons is above a certain threshold, among others. These experiments offer a proof of concept that the network is able to learn by using exact gradients. We hope our work will provide a rigorous stepping stone for developing or improving a training library for SNNs.

Table 3 describes the hyperparameters used for training the SNN on the Yin-Yang dataset. The hyperparameters were chosen by a manual search through several combinations of the architecture and the parameters shown in the table. The final experiments were done on machines part of an internal cluster with 48 CPU and 5 GB memory, which results in training over 300 full epochs through the entire training dataset of 5000 examples and evaluation on the entire test dataset of 1000 examples completing in approximately 3 hours.

methods, instead we used both a spike count-based cross entropy loss and a spike rate cross entropy loss. The former calculates cross entropy from the number of spikes emitted by output neurons, with the network learning to fire more at the label neuron, and the latter accumulates cross entropy loss at each time step, with the network learning to fire continuously at the label neuron and others to be silent.

Table 1: Hyperparameters for XOR Task

SYMBOL	DESCRIPTION	VALUE
$\alpha = \frac{1}{\tau_s}$	Inverse synaptic time constant	1.0
$\beta = \frac{1}{\tau_n}$	Inverse membrane time constant	0.99
θ	Threshold	1.0
T	Maximum time	2.0
t_{early}	Minimum time	0.0
	Hidden sizes	[4]
	Hidden weights mean	[3.0]
	Hidden weights stdev	[1.0]
	Output weights mean	2.0
	Ouput weights stdev	0.1
	Optimizer	Adam
β_1	Adam parameter	0.9
β_2	Adam parameter	0.999
ϵ	Adam parameter	$1e-8$
η	Learning rate	0.1
γ	Regularization factor	0.2
τ_0	First loss time constant	0.1
τ_1	Second loss time constant	1.0

Table 2: Hyperparameters for Iris Classification

SYMBOL	DESCRIPTION	VALUE
$\alpha = \frac{1}{\tau_s}$	Inverse synaptic time constant	1.0
$\beta = \frac{1}{\tau_n}$	Inverse membrane time constant	0.9
θ	Threshold	1.0
T	Maximum time	16.0
t_{early}	Minimum time	0.0
	Hidden sizes	[10]
	Hidden weights mean	[3.0]
	Hidden weights stdev	[1.0]
	Output weights mean	2.0
	Ouput weights stdev	0.1
	Optimizer	Adam
β_1	Adam parameter	0.9
β_2	Adam parameter	0.999
ϵ	Adam parameter	$1e-8$
η	Learning rate	0.05
γ	Regularization factor	0.1
τ_0	First loss time constant	1.0
τ_1	Second loss time constant	1.0

Table 3: Hyperparameters for Yin-Yang Simulations

SYMBOL	DESCRIPTION	VALUE
$\alpha = \frac{1}{\tau_s}$	Inverse synaptic time constant	0.999
$\beta = \frac{1}{\tau_n}$	Inverse membrane time constant	1.0
θ	Threshold	1.0
T	Maximum time	2.0
t_{early}	Minimum time	0.15
t_{bias}	Bias time	0.9
	Hidden sizes	[150]
	Hidden weights mean	[1.5]
	Hidden weights stdev	[0.8]
	Output weights mean	2.0
	Ouput weights stdev	0.1
	Minibatch size	150
	Epochs	300
	Optimizer	Adam
β_1	Adam parameter	0.9
β_2	Adam parameter	0.999
ϵ	Adam parameter	$1e-8$
η	Learning rate	0.0005
γ	Regularization factor	0.005
τ_0	First loss time constant	0.2
τ_1	Second loss time constant	1.0